Journal of Applied Polymer Science

Sorption/release of diclofenac sodium in/from free-standing poly(acrylic acid)/poly(ethyleneimine) multilayer films

Claudiu-Augustin Ghiorghita, Florin Bucatariu, Ecaterina Stela Dragan
"Petru Poni" Institute of Macromolecular Chemistry, Aleea Grigore Ghica Voda 41A, Iasi 700487, Romania
Correspondence to: E. S. Dragan (E-mail: sdragan@icmpp.ro)

ABSTRACT: Polyelectrolyte multilayer films deposited onto various substrates have been used extensively as drug delivery systems. However, little attention has been paid to the release of drugs from free-standing polymeric films. Herein, we report the construction of thermal crosslinked free-standing poly(acrylic acid) (PAA)/branched poly(ethyleneimine) (PEI) multilayer films composed of 25 double layers [$(PAA/PEI)_{25}$] and their use in sorption/release of diclofenac sodium (DS). The $(PAA/PEI)_{25}$ multilayer films were characterized by scanning electron microscopy, potentiometric titrations and Fourier transform infrared spectroscopy, while the sorption/release of DS was monitored by UV–Vis spectroscopy. The DS sorption equilibrium data were fitted with five isotherm models (Langmuir, Freundlich, Sips, Dubinin–Radushkevich, and Temkin). The maximum equilibrium sorption capacity, q_m, given by the Langmuir model was 32.42 mg DS/g. The Korsmeyer–Peppas semiempirical equation showed that the release of DS from the free-standing $(PAA/PEI)_{25}$ films proceeded by pseudo-Fickian diffusion, irrespective of the releasing media. © 2016 Wiley Periodicals, Inc. J. Appl. Polym. Sci. **2016**, *133*, 43752.

KEYWORDS: adsorption; drug delivery systems; films; polyelectrolytes; self-assembly

Received 11 February 2016; accepted 5 April 2016
DOI: 10.1002/app.43752

INTRODUCTION

Fabrication of thin polymeric films has been of considerable importance in both industrial and fundamental research due to their potential applications in various areas, such as packaging,[1] protective coatings,[2] modern microelectronics,[3,4] smart actuators,[5] battery separators,[6] antibacterial and antifouling films,[7,8] biocompatible membranes for drug delivery,[9,10] or tissue engineering.[11] Among the methods used to design polymeric films, layer-by-layer (LbL) assembly strategy is very attractive due to its versatility and the large number of building-blocks (synthetic and natural polyelectrolytes, inorganic nanoparticles, biomolecules, dyes, etc.), which can be used in the deposition process.[12–16] Also, the properties of multilayer films are influenced by the assembly conditions, such as the concentration, pH, ionic strength and temperature of deposition solutions.[17–24] All these parameters allowed the design of a large variety of multilayer films, which have found applications as separation membranes,[25,26] anticorrosion, and flame-retardant coatings,[27,28] antimicrobial membranes,[29,30] drug delivery systems,[31–35] etc.

Recently, the LbL strategy has been used to construct free-standing polymeric films. The main approaches employed to obtain free-standing multilayer films consisted in either the deposition of the films directly on to a substrate with low surface energy, followed by their gently exfoliation,[36–38] or the deposition of a sacrificial layer inserted between the films and the substrate, which afterwards can be removed in appropriate conditions.[39–42] Sacrificial layers are usually stimuli responsive polymers, which change their properties as a function of pH, ionic strength, solvent, or temperature. Ji *et al.* constructed free-standing multilayer films using cellulose acetate as sacrificial layer, which was afterwards dissolved in acetone.[39] Schlenoff *et al.* studied the formation of free-standing multilayer films using pairs of poly(acrylic acid) (PAA)/poly(diallyldimethyl ammonium chloride) (PDADMAC) as sacrificial layers, which were decomposed in saline solution with different pH values.[40] Sun *et al.* used PDADMAC as sacrificial layer for the construction of free-standing PAA/poly(allylamine hydrochloride) (PAH) multilayer films, which was removed in acidic aqueous solution (pH 2) after the film formation.[41,42]

Multilayer films have been intensively investigated as potential drug delivery systems for a large variety of low and high molar mass bioactive compounds.[31–35] However, in many studies the films were directly attached to the underlying substrate, this being a disadvantage for large scale applications, either because the substrate is nondegradable in living organisms, or because its degradation products are often toxic. The free-standing multilayer films could overcome these drawbacks and also might lead to the development of new drug delivery systems, such as transdermal patches.[43]

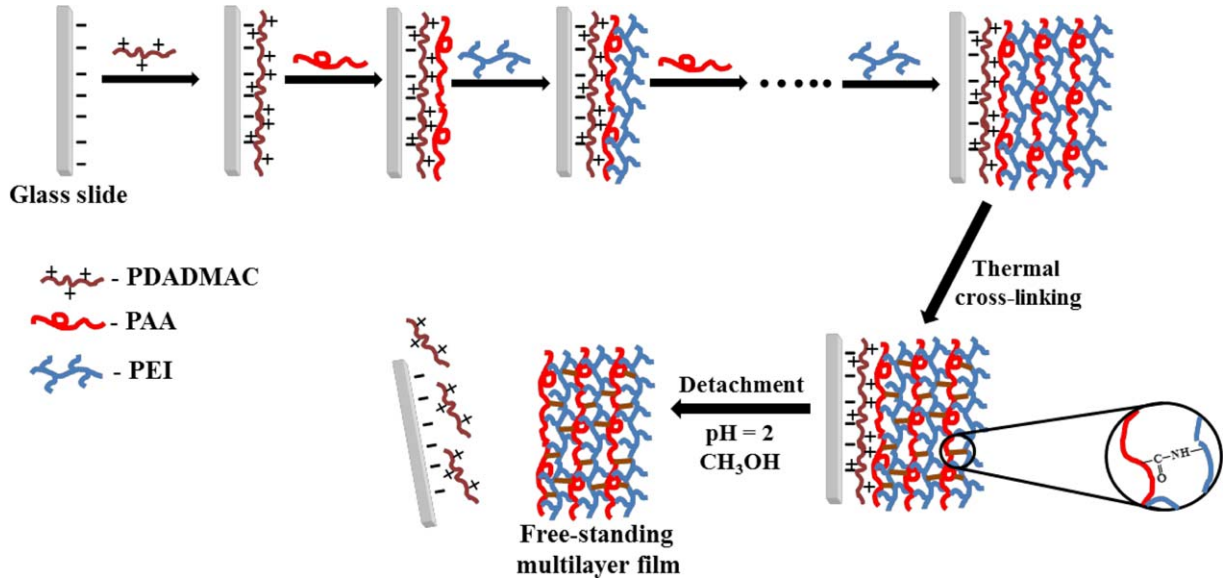

Figure 1. Schematic representation for the deposition, crosslinking, and detachment steps of free-standing $(PAA/PEI)_{25}$ multilayer film. [Color figure can be viewed in the online issue, which is available at wileyonlinelibrary.com.]

Therefore, the main objective of this study was to investigate the mechanisms of sorption and release of diclofenac sodium (DS) in/from PAA/PEI free-standing multilayer films. The detachment of the PAA/PEI multilayers films from the underlying substrate was performed using an original procedure involving a mixt pH and solvent treatment. The free-standing films were characterized by scanning electron microscopy (SEM), potentiometric titrations, and Fourier transform infrared (FT-IR) spectroscopy, while the sorption/release capacity for DS was determined by UV–vis spectroscopy. The sorption/release mechanisms of DS in/from the free-standing PAA/PEI films were deeply investigated by fitting the sorption/release data with various mathematical models.

EXPERIMENTAL

Materials

Branched poly(ethyleneimine) (PEI, M_w = 25,000 g mol^{-1}), poly (acrylic acid) (PAA, 35% aqueous solution, M_w = 100,000 g mol^{-1}) and DS were purchased from Sigma Aldrich (St. Louis, Missouri) and were used without further purification. PDADMAC (M_w = 240,000 g mol^{-1}) was purchased from Polysciences (Warrington, PA, USA) and used without purification. Microscope glass slides with sizes of 76 mm × 26 mm × 1 mm (height × width × thickness) were acquired from Menzel–Gläser, Thermo Fisher Scientific (Braunschweig, Germany) and used as received. For all experiments, Millipore-grade water with a conductivity of 0.055 μS m^{-1} was used.

Construction of PAA/PEI Multilayer Films and Their Detachment from Glass Substrate

The PAA/PEI multilayer films were constructed on to microscope glass slides using an automated dipping device ND-R Rotatory Dip Coater (Nadetech Innovations S.L., Navarra, Spain). The entire deposition procedure, as well as the crosslinking and detachment steps used for the construction of free-standing $(PAA/PEI)_{25}$ multilayer films is illustrated in Figure 1. Prior to multilayer deposition, the glass slides were cleaned by immersing in freshly prepared Piranha solution [a 70:30% (v/v) mixture of H_2SO_4:H_2O_2] for 60 min (Caution! Piranha solution is highly corrosive and should be handled with extreme care.), followed by intensive rinsing with water. After the cleaning stage, the glass slides were immersed for 30 min in PDADMAC solution ($C_{PDADMAC}$ = 10^{-2} mol L^{-1}) to deposit the sacrificial polymeric layer. Next, the PAA/PEI multilayer film was assembled onto the glass slides covered with the PDADMAC layer. The substrates were first immersed in PAA solution (C_{PAA} = 10^{-2} mol L^{-1}, pH = 3.5) for 15 min, followed by three rinsing steps with water, each 1 min. Then, the substrates were immersed in PEI solution (C_{PEI} = 10^{-2} mol L^{-1}, pH = 9.5) for 15 min, followed by three rinsing steps with water, each 1 min. This procedure describes the assembly of one PAA/PEI double layer. These steps were repeated until 25 double layers have been deposited onto the PDADMAC modified glass slides; hereafter, this multilayer film was defined as $(PAA/PEI)_{25}$.

After the deposition of the $(PAA/PEI)_{25}$ multilayer, the film was thermally crosslinked in an oven for 3 h at 140 °C. Before detachment, the edges of the glass slides covered with the $(PAA/PEI)_{25}$ multilayer film have been scratched with a razorblade. Then, the glass slides were immersed for 30 min in an aqueous solution of HCl with pH 2, and afterwards in methanol. This procedure allowed the exfoliation of two flawless free-standing $(PAA/PEI)_{25}$ multilayer films, one from each side of the glass slide.

Characterization Methods

The chemical composition of the free-standing $(PAA/PEI)_{25}$ film was studied by FT-IR spectroscopy in transmission mode using a Bruker Vertex 70 spectrophotometer at frequencies ranging from 4000 to 400 cm^{-1}. Samples of free-standing films were crumbled into a mortar, and then the powder was mixed with KBr and pressed into pellets.

The thickness of the free-standing $(PAA/PEI)_{25}$ film was evaluated by SEM using an Environmental Scanning Electron

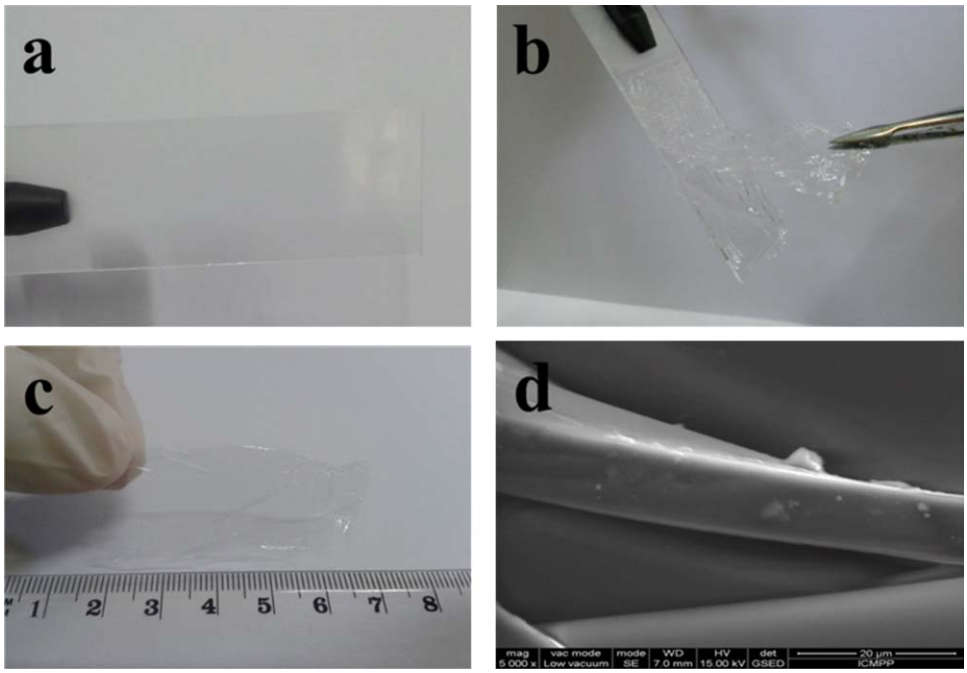

Figure 2. Optical images of the $(PAA/PEI)_{25}$ film: (a) before detachment, (b) its exfoliation after the immersion in detachment solutions, and (c) the image of a completely detached film. Cross-sectional SEM image of the free-standing $(PAA/PEI)_{25}$ film (d). [Color figure can be viewed in the online issue, which is available at wileyonlinelibrary.com.]

Microscope (ESEM) type Quanta 200, operating at 15 kV with secondary electrons, in low vacuum mode.

Potentiometric titrations were performed with a PCD 03 (Mütek, Germany) particle charge detector, between pH 3 and 10, using 0.01 mol L^{-1} HCl and NaOH, respectively. The potentiometric titrations were used to determine the point of zero charge (*pzc*) of the free-standing $(PAA/PEI)_{25}$ film, which is defined as the numeric value of pH where the potential is zero mV.

The optical images of the $(PAA/PEI)_{25}$ film before, during and after detachment from the glass slides were acquired using a Nikon Coolpix S3000 digital camera, at a resolution of 12 MP.

Sorption and Release of Diclofenac Sodium

The sorption/release experiments of DS in/from the free-standing PAA/PEI multilayer films were performed by a batch procedure, at room temperature. For the sorption isotherm, the $(PAA/PEI)_{25}$ films were immersed for 2 h in a predetermined volume of DS aqueous solution, to keep a constant ratio of 1 mg film/1 mL of DS solution. The adsorbed amount of DS (q_e, mg g^{-1}) was determined using eq. (1):

$$q_e = \frac{(C_0 - C_e)V}{m} \times 10^3 \quad (1)$$

where C_0 and C_e represent the concentration of DS in the aqueous solution (mg L^{-1}) before and after the interaction with the multilayer film, V is the volume of DS solution (mL) and m is the multilayer film weight (mg).

In vitro release of DS from the $(PAA/PEI)_{25}$ film was performed in phosphate buffered saline (PBS) solution and in NaOH aqueous solutions with pH 8 and pH 10 by immersing the free-standing films loaded with DS in 10 mL release medium. At predetermined time intervals, 2 mL of desorption solution were withdrawn and analyzed by UV–Vis spectroscopy using a SPECORD 200 Plus Analytic Jena spectrophotometer (Germany). The removed solution was replaced with an identical volume of fresh releasing media to keep the volume constant. The cumulative release of DS was calculated using eq. (2):

$$\%\ \text{DS (released)} = \frac{(10C_n + 2\sum C_{n-1})}{m_0} \times 100 \quad (2)$$

where C_n and C_{n-1} are the concentrations of DS (mg L^{-1}) in the releasing medium after n and $n-1$ withdrawing steps, respectively; n is the number of withdrawing steps of releasing media; m_0 is the amount of DS (mg) loaded by the multilayer films.

RESULTS AND DISCUSSION

$(PAA/PEI)_{25}$ multilayer films were deposited onto glass slides, which were previously coated with a layer of PDADMAC using the procedure described in Figure 1. The pH of the deposition solutions (pH_{PAA} = 3.5 and pH_{PEI} = 9.5) was chosen so because both polyelectrolytes were only partially ionized. Therefore, the driving forces which lead to the assembly of the multilayer film were the formation of electrostatic interactions between the COO^- groups of PAA and NH_3^+ groups of PEI, as well as the hydrogen bonding between the protonated carboxylic acid groups of PAA and amino groups of PEI. In this way both polyelectrolytes adopt a coiled conformation, which leads to thick deposited layers. After the $(PAA/PEI)_{25}$ multilayer film was completely formed, its detachment from the underlying substrate was performed as presented previously. Figure 2 shows the optical images of a $(PAA/PEI)_{25}$ film deposited on to glass slides before detachment (a), its exfoliation after the immersion in detachment solutions (b) and the image of a completely detached film (c).

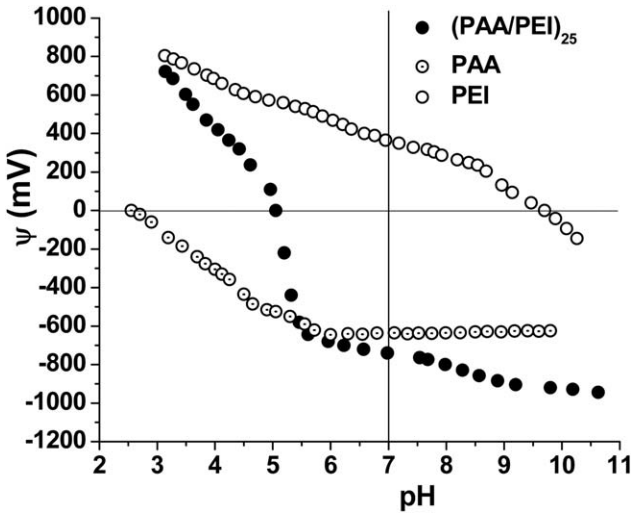

Figure 3. Potentiometric titrations of PAA, PEI, and $(PAA/PEI)_{25}$ free-standing film.

Before detachment, the surface of the glass slides covered with the $(PAA/PEI)_{25}$ film was smooth [Figure 2(a)]. After the immersion in the HCl solution with pH 2, the film began to detach from the surface of the underlying substrate due to the cleavage of electrostatic interactions between the underlying PDADMAC sacrificial layer and the first deposited PAA layer. The detachment process proceeded slowly, the $(PAA/PEI)_{25}$ multilayer film being almost completely detached after 30 min. Then, the glass slide was gently removed from the pH 2 solution and immersed in methanol for 1 min. This led to the dehydration of the film, which afterwards was easily exfoliated from the glass slide [Figure 2(b)]. Figure 2(c) shows the image of a completely detached, flawless $(PAA/PEI)_{25}$ multilayer film. Furthermore, the thickness of the free-standing $(PAA/PEI)_{25}$ film was evaluated using SEM [Figure 2(d)]. The cross-sectional SEM image shows that the film was uniformly deposited and that the detachment procedure did not produce defects in its structure. The thickness of the $(PAA/PEI)_{25}$ film, evaluated using the ImageJ software, was estimated at 11 ± 0.2 μm, which is in agreement with other literature reports on multilayer films constructed using this pair of polyelectrolytes.[37]

To gain information about the balance of charged groups inside the $(PAA/PEI)_{25}$ film, potentiometric measurements were performed on to $(PAA/PEI)_{25}$ particles (obtained by the mechanical destruction of the solid film). For comparison, PAA and PEI titrations were carried out independently (Figure 3).

As can be observed in Figure 3, the point of zero charge (*pzc*) of the film is situated at pH 5.04. This value of *pzc*, located in the acidic range of pH, indicates that the carboxylic groups are in a little excess in the $(PAA/PEI)_{25}$ free-standing film than amino groups from the PEI. Because the deposition pH of PAA solution was 3.5 and for PEI solution 9.5, they were adsorbed in a coiled conformation. Therefore, the polyelectrolyte with a higher molar mass, which is PAA (M_w = 100.000 g mol^{-1}), will form layers of coiled chains where some carboxylic groups could be not overcompensated by the amino groups of the PEI branched chains. On the other hand, the positively charged centers distributed on the PEI chains could not be all involved in electrostatic interactions. Probably the number of carboxylic groups was higher than that of amino groups and thus the *pzc* of the $(PAA/PEI)_{25}$ film was located in the acidic range of pH.

Sorption/Release of DS

Although the $(PAA/PEI)_{25}$ free-standing film had a *pzc* in acidic range of pH, it was able to sorb DS, a negatively charged drug, by interacting with protonated amino groups from PEI layers (mainly with the last deposited layer). Another factor which can influence the sorption of DS by the free-standing film could be the loose nature of PEI layers, the conformation of PEI chains being less compact than that of the linear PAA chains.

The capacity of the PAA/PEI multilayer films to interact with DS was first assessed by FT-IR measurements. Figure 4 presents the FT-IR spectra of the free-standing $(PAA/PEI)_{25}$ film, before and after its interaction with DS.

The FT-IR spectrum of pristine $(PAA/PEI)_{25}$ film [Figure 4(a)] was in agreement with the spectrum presented in literature for this system.[44] Important peaks were observed at 1720, 1560, and 1404 cm^{-1}, the first being assigned to the stretching vibrations of C═O bonds in COOH groups, and the next two to the asymmetric and symmetric stretching vibrations of COO^- groups from PAA sodium salt, respectively. The peak at 1618 cm^{-1} was attributed to the deformation vibrations of NH groups in PEI chains, while the peak at 1450 cm^{-1} was assigned to the deformation vibrations of CH_2 groups belonging to both polymers. By

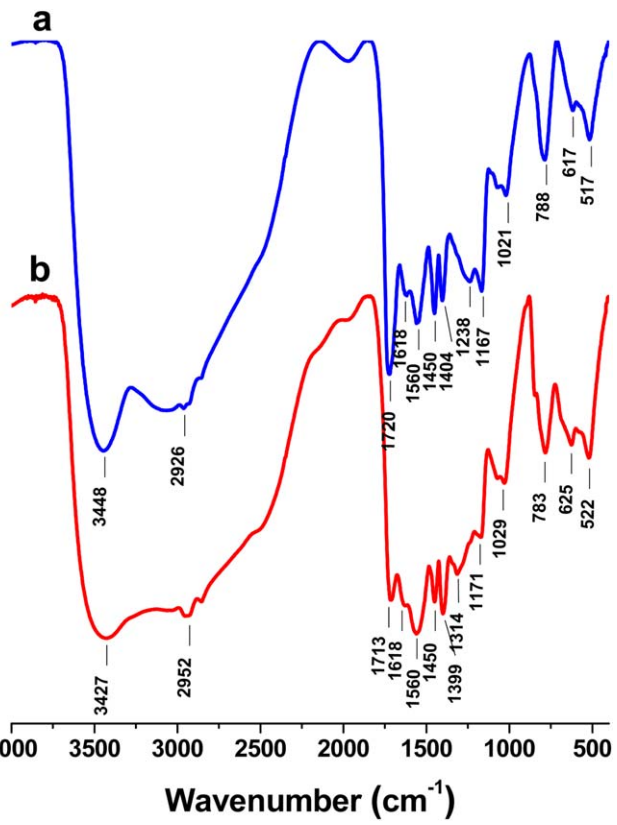

Figure 4. FT-IR spectra of free-standing $(PAA/PEI)_{25}$ multilayer film (a) before and (b) after sorption of DS. [Color figure can be viewed in the online issue, which is available at wileyonlinelibrary.com.]

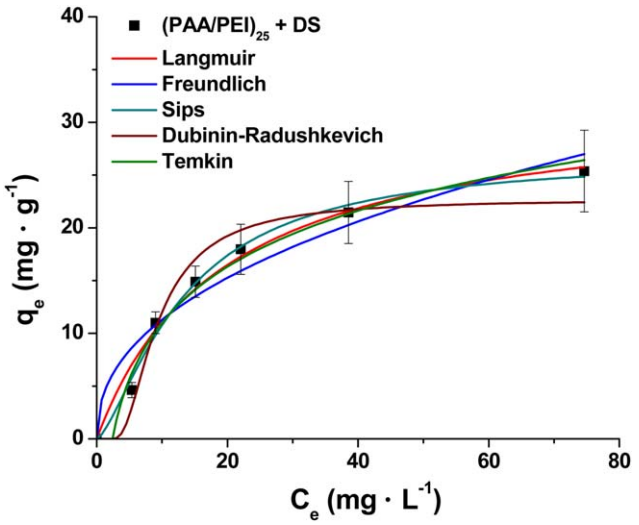

Figure 5. Equilibrium adsorption isotherm for the sorption of DS by the free-standing $(PAA/PEI)_{25}$ multilayer film. [Color figure can be viewed in the online issue, which is available at wileyonlinelibrary.com.]

comparing the spectrum of pristine $(PAA/PEI)_{25}$ film with the spectrum of the film loaded with DS [Figure 4(b)], a new peak was observed at 1314 cm^{-1}, which was attributed to the stretching vibrations of C—O bonds belonging to COO^- groups of DS, thus demonstrating the successful incorporation of DS inside the multilayer film. Moreover, the peaks at 1720 cm^{-1} (—COOH) and 1560 cm^{-1} ($—COO^-$) were used to investigate the PAA/PEI complexation inside the multilayer film, before and after its interaction with DS. In the spectrum of pristine $(PAA/PEI)_{25}$ film, the intensity of —COOH peak is higher than the intensity of $—COO^-$, indicating that the hydrogen bonding inside the multilayer is more pronounced than the ionic interactions. However, after the sorption of DS, the hydrogen bonding/ionic interactions equilibrium inside the multilayer film changed significantly, the $—COO^-$ peak being more intense than —COOH. The increased intensity of the 1560 cm^{-1} peak was attributed to the presence of asymmetrical stretching vibrations of $—COO^-$ groups from both PAA and DS.

In order to determine the maximum adsorption capacity for DS of the free-standing $(PAA/PEI)_{25}$ film, the sorption isotherm was constructed (Figure 5).

The shape of the experimental isotherm indicates a "*L*" type isotherm, where the representation of the concentration of DS remained in solution as a function of the amount of DS adsorbed by the $(PAA/PEI)_{25}$ multilayer film is a concave curve.[45] The experimental results were fitted with five isotherm models (Langmuir, Freundlich, Sips, Dubinin–Radushkevich, and Temkin) to establish the most appropriate model which describes the sorption process. The nonlinear forms of the isotherm models and their parameters are presented below.

The Langmuir isotherm is described by eq. (3)[46]:

$$q_e = \frac{q_m K_L C_e}{1 + K_L C_e} \tag{3}$$

where q_m is the maximum adsorption capacity when the surface is fully covered with a monolayer of sorbate molecules (mg g^{-1}) and K_L is the Langmuir constant (L mg^{-1}), which is related to the energy of adsorption. The value of K_L can be used to assess the feasibility of the adsorption process by calculating the dimensionless constant R_L, which is called "constant separation factor" or "equilibrium parameter". Its expression is given by eq. (4)[47]:

$$R_L = \frac{1}{1 + K_L C_i} \tag{4}$$

where K_L is the Langmuir adsorption constant (L mg^{-1}) and C_i is the highest initial concentration of the sorbate (mg L^{-1}). If $R_L > 1$, the sorption process is unfavorable, if $R_L = 1$ the sorption process is linear, if $0 < R_L < 1$ the sorption is favorable, and if $R_L = 0$, then the sorption process is irreversible.

The Freundlich isotherm is described by eq. (5)[48]:

$$q_e = K_F C_e^{1/n} \tag{5}$$

where K_F is the Freundlich constant, which estimates the amount of sorbate retained per gram of sorbent at the equilibrium concentration (mg g^{-1}) and n is a measure of the nature and strength of the adsorption process and the distribution of active sites related to the surface heterogeneity (the heterogeneity of the system increases with n).

The Sips isotherm is described by eq. (6)[49]:

$$q_e = \frac{q_m a_S C_e^{1/n}}{1 + a_S C_e^{1/n}} \tag{6}$$

where q_m is the monolayer adsorption capacity (mg g^{-1}), a_S is the Sips constant related to the energy of adsorption. Also, *1/n* values close to zero indicate that the sorbent is heterogeneous, while values closer to 1 indicate relatively homogeneous distribution of binding sites.

The Dubinin–Radushkevich isotherm is given by eq. (7)[50]:

$$q_e = q_{DR} \exp\left\{-\beta\left[RT \ln\left(1 + \frac{1}{C_e}\right)\right]^2\right\} \tag{7}$$

where q_{DR} is the maximum adsorption capacity (mg g^{-1}) and β is the Dubinin–Radushkevich constant (mol^2 kJ^{-2}).

The Temkin isotherm is described by eq. (8)[51]:

$$q_e = \frac{RT}{b_T} \ln a_T C_e \tag{8}$$

where b_T is the Temkin constant related to the thermal behavior of the sorption process (kJ mol^{-1}) and a_T is the equilibrium binding constant corresponding to the maximum binding energy (L mg^{-1}).

The statistical analysis of errors was performed by means of correlation coefficient of determination (R^2) and by the nonlinear Chi-square test (χ^2), which is mathematically expressed by eq. (9):

$$\chi^2 = \sum \frac{(q_{e,exp} - q_{e,cal})^2}{q_{e,cal}} \tag{9}$$

where $q_{e,exp}$ and $q_{e,cal}$ represents the experimental and calculated adsorption capacity of the composites (mg g^{-1}).

The adsorption isotherm parameters for the sorption of DS by the free-standing $(PAA/PEI)_{25}$ films, as well as the correlation

Table I. Isotherm Parameters of Langmuir, Freundlich, Sips, Dubinin–Radushkevich, and Temkin Models Obtained by Nonlinear Fitting for the Sorption of DS on to $(PAA/PEI)_{25}$ Multilayer Film

Isotherm model	Parameters	$(PAA/PEI)_{25}$ + DS
Langmuir	q_m (mg g^{-1})	32.42
	K_L (L mg^{-1})	5.17×10^{-2}
	R_L	0.162
	R^2	0.982
	χ^2	1.50
Freundlich	K_F (mg g^{-1})	4.17
	$1/n$	0.43
	R^2	0.936
	χ^2	5.26
Sips	q_m (mg g^{-1})	26.89
	a_S	2.41×10^{-2}
	$1/n$	1.44
	R^2	0.989
	χ^2	0.90
Dubinin–Radushkevich	q_{DR} (mg g^{-1})	22.71
	β (mol^2 kJ^2)	1.14×10^{-5}
	R^2	0.952
	χ^2	3.94
Temkin	a_T (L mg^{-1})	315.57
	b_T (J mol^{-1})	0.42
	R^2	0.986
	χ^2	1.15

coefficients (R^2) and noninear Chi-square test (χ^2), obtained by the nonlinear regression method are presented in Table I.

The values of the isotherm parameters show that the results were fitted better by the Langmuir, Sips, and Temkin models, in these cases the R^2 values being higher and χ^2 values lower than the ones obtained for Freundlich and Dubinin–Radushkevich model isotherms. The Langmuir isotherm is applicable to homogeneous adsorption where all the adsorption sites are assumed to be identical, each site retains one molecule of the given compound, and all sites are energetically independent of the adsorbed quantity. The high degree of fitting of the experimental data by the Langmuir isotherm model indicates that the sorption of DS was homogeneous and that the ionic groups were uniformly distributed on the surface and inside of the free-standing films. Also, the R_L value calculated using eq. (5) for the adsorption of DS on to the $(PAA/PEI)_{25}$ multilayer film was 0.162, indicating that the sorption process is favorable. Moreover, the fitting of experimental data by the Sips isotherm shows that the active sites are homogeneously distributed on the surface as well as inside the multilayer film.[52]

Similar studies regarding the sorption mechanism of bioactive compounds by multilayer films have been previously performed, but in all cases the films were not detached from the underlying substrate.[33,34] To the best of our knowledge, this is the first study which investigated the sorption mechanism of bioactive compounds by free-standing multilayer films. However, the shape of the isotherm and the best isotherm models which fit the experimental data for the free-standing PAA/PEI film are in agreement with the results obtained for other types of multilayer films undetached from the substrate. This behavior could be attributed to the asymmetry of film faces, the sorption of DS taking place only through the face of the films covered with PEI, while the face covered with PAA repels the drug molecules.

The release of DS from the free-standing $(PAA/PEI)_{25}$ multilayer film was investigated in PBS (pH = 7.4) solution, and in NaOH solutions with pH 8 and 10 (Figure 6).

The release of DS in PBS solution was fast in the first 50 min, while afterwards it almost stopped. When the release was studied in pH 8 and pH 10 solutions, the initial fast regime lasted approximately 100 min, and afterwards it slowed down significantly. In all cases, the initial fast regime was attributed to the release of drug molecules sorbed near the external surface of the film. Also, it can be seen that the percentage of DS released from the free-standing $(PAA/PEI)_{25}$ film slightly increased with increasing the pH of the media. DS is an anionic molecule ($pK_a \approx 4.2$), which interacts with the free-standing film through electrostatic interaction with the amine groups of the polycation. PEI is a weakly charged polycation ($pzc \approx 9.7$), its ionization degree being influenced by the pH of the environment. In pH 10, a lower number of amino groups are ionized than at pH 8, thus explaining the releasing of a slightly higher percentage of DS. However, as the shape of the cumulative release shows, the release at pH 8 could lead to higher percentage of DS released at longer desorption times. Although the pH of the PBS solution is 7.4, it also contains a large amount of inorganic salts (NaCl, KCl, NaH_2PO_4, and K_2HPO_4), which are screening the interaction between DS and the multilayer film, thus favoring the release of the drug molecules.

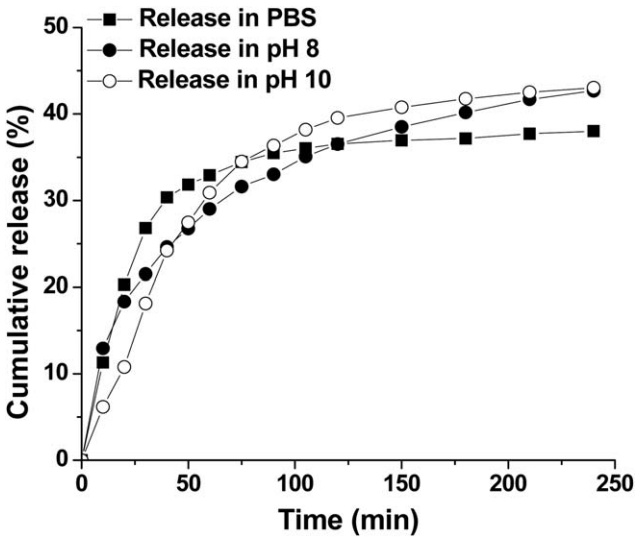

Figure 6. Cumulative release of DS from the free-standing $(PAA/PEI)_{25}$ film in PBS (filled squares), pH 8 (filled circles) and pH 10 (empty circles) solutions.

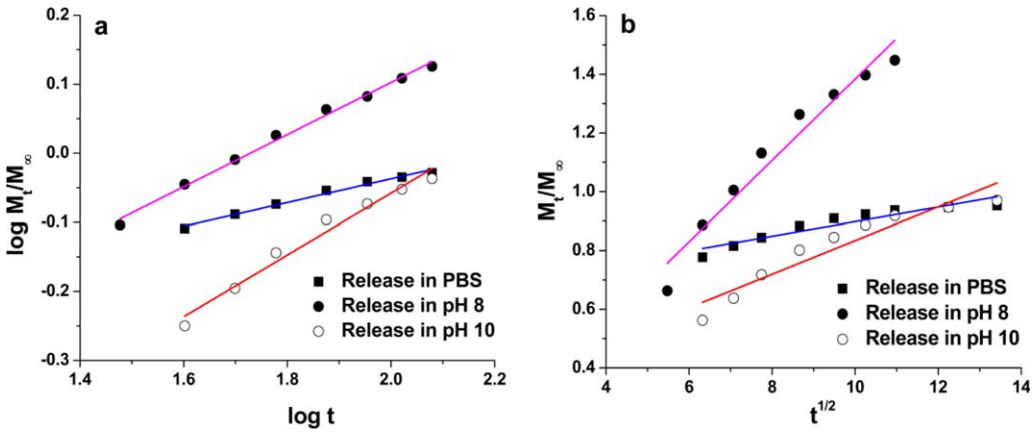

Figure 7. Linear forms of Korsmeyer–Peppas (a) and Higuchi (b) models applied for the release of DS from free-standing $(PAA/PEI)_{25}$ multilayer film in PBS (filled squares), pH = 8 (filled circles) and pH = 10 (empty circles) solutions. [Color figure can be viewed in the online issue, which is available at wileyonlinelibrary.com.]

To obtain information about the release mechanism, the data regarding the release of DS from the free-standing $(PAA/PEI)_{25}$ film were kinetically analyzed using Korsmeyer–Peppas and Higuchi semiempirical models, which were applied for the initial stages of release ($\sim$ 60% of fractional release). The Korsmeyer–Peppas model describes the release of drugs using eq. (10)[53,54]:

$$\frac{M_t}{M_\infty} = kt^{n_r} \tag{10}$$

where M_t/M_∞ represents the fraction of the released drug, M_t and M_∞ are the cumulative amounts of DS released at time t and at infinite time (the maximum released amount), respectively, k is a constant related to the matrix and the exponent n_r gives information about the release mechanism. Values of $n_r \leq 0.5$ indicate a Fickian diffusion mechanism, while when $0.5 < n_r < 1$ the drug release proceeds through an anomalous or non-Fickian mechanism. A case II mechanism of transport is suggested when $n_r = 1$, and a special case II release mechanism is involved when $n_r > 1$.

The Higuchi model uses eq. (11) to describe the release of drugs from polymeric systems[55]:

$$\frac{M_t}{M_\infty} = kt^{1/2} \tag{11}$$

where M_t/M_∞, M_t and M_∞ have the same significance as above, and k is the Higuchi constant.

Table II. Parameters of Korsmeyer–Peppas and Higuchi Models Obtained by Linear Fitting for the Release of DS from the Free-Standing $(PAA/PEI)_{25}$ Film

Release conditions	Korsmeyer–Peppas model		Higuchi model	
	n_r	R^2	K	R^2
PBS (pH 7.4)	0.171	0.983	0.025	0.875
pH 8	0.378	0.993	0.138	0.949
pH 10	0.447	0.970	0.057	0.899

The linear forms of the Korsmeyer-Peppas and Higuchi equations fitted on the release data of DS from the free-standing $(PAA/PEI)_{25}$ multilayer film were plotted in Figure 7. The main parameters obtained after fitting the release of DS from the free-standing $(PAA/PEI)_{25}$ film with the Korsmeyer–Peppas and Higuchi equations are presented in Table II.

The release of DS from the free-standing $(PAA/PEI)_{25}$ multilayer film was better described by the Korsmeyer–Peppas model, the correlation coefficients being higher than in the case of Higuchi model. The n_r parameter obtained for all release conditions was lower than 0.5, which indicate that the release of DS from free-standing $(PAA/PEI)_{25}$ film proceeds by pseudo-Fickian diffusion mechanism. In the case of Higuchi model, the plots M_t/M_∞ versus $t^{1/2}$ for all release conditions are nonlinear, therefore this model cannot be used to accurately describe de release of DS from the $(PAA/PEI)_{25}$ film.

CONCLUSIONS

In this study, we demonstrated that free-standing PAA/PEI multilayer films can be obtained using a detachment procedure involving a mixt pH and solvent treatment. The exfoliated films were defect-free and thick enough (11 $\pm$ 0.2 μm) to be easily handled. Although the potentiometric measurements showed that the PAA/PEI multilayers contained a higher number of carboxylic groups, the free-standing films successfully sorbed DS, an anionic drug. The sorption isotherm showed that the amount of DS sorbed by the free-standing PAA/PEI films increased with increasing the equilibrium concentration. The Langmuir, Sips, and Temkin models fitted well the equilibrium sorption data, the maximum equilibrium sorption capacity, q_m, estimated by the Langmuir model being 32.42 mg DS/g. The release of DS was initially fast due to the desorption of drug molecules loaded onto the external surface of the film, slowing down afterwards as the drug molecules loaded inside the multilayer were released. The Korsmeyer–Peppas semiempirical equation showed that the release proceeded by pseudo-Fickian diffusion mechanism.

ACKNOWLEDGMENTS

This work was supported by a grant of the Romanian National Authority for Scientific Research, CNCS UEFISCDI, project number PN-II-ID-PCE-2011-3-0300.

REFERENCES

1. Barlow, C. Y.; Morgan, D. C. *Resour. Conserv. Recycl.* **2013**, *78*, 74.
2. Wang, N.; Xiong, D.; Deng, Y.; Shi, Y.; Wang, K. *ACS Appl. Mater. Interfaces* **2015**, *7*, 6260.
3. Peng, X.; Wu, Q.; Jiang, S.; Hanif, M.; Chen, S.; Hou, H. *Mater. Lett.* **2014**, *133*, 240.
4. Xu, W.; Ding, Y.; Jiang, S.; Ye, W.; Liao, X.; Hou, H. *Polym. Compos.* **2016**, *37*, 794.
5. Jiang, S.; Liu, F.; Lerch, A.; Ionov, L.; Agarwal, S. *Adv. Mater.* **2015**, *27*, 4865.
6. Ye, W.; Zhu, J.; Liao, X.; Jiang, S.; Li, Y.; Fang, H.; Hou, H. *J. Power Sources* **2015**, *299*, 417.
7. Zhang, M.; Yang, F.; Pasupuleti, S.; Oh, J. K.; Kohli, N.; Lee, I. S.; Perez, K.; Verkhoturov, S. V.; Schweikert, E. A.; Jayaraman, A.; Cisneros-Zevallos, L.; Akbulut, M. *Int. J. Food Microbiol.* **2014**, *185*, 73.
8. Zhang, W.; Vinueza, N. R.; Datta, P.; Michielsen, S. *J. Polym. Sci. A: Polym. Chem.* **2015**, *53*, 1594.
9. Fox, C. B.; Kim, J.; Le, L. V.; Nemeth, C. L.; Chirra, H. D.; Desai, T. A. *J. Control. Release* **2015**, *219*, 431.
10. Hu, X.; Gong, X. *J. Colloid Interface Sci.* **2016**, *470*, 62.
11. Suntornnond, R.; An, J.; Yeoung, W. Y.; Chua, C. K. *Macromol. Mater. Eng.* **2015**, *300*, 858.
12. Decher, G. *Science* **1997**, *277*, 1232.
13. Crouzier, T.; Boudou, T.; Picart, C. *Curr. Opin. Colloid Interface Sci.* **2010**, *15*, 417.
14. Dragan, E. S.; Schwarz, S.; Eichhorn, K. J. *Colloids Surf. A* **2010**, *372*, 210.
15. Fadhillah, F.; Zaidi, S. M. J.; Khan, Z.; Khaled, M.; Rahman, F.; Hammond, P. *J. Appl. Polym. Sci.* **2012**, *126*, 1468.
16. Doan, T.; Day, R.; Leopold, M. *J. Mater. Sci.* **2012**, *47*, 108.
17. Gao, C.; Gong, X. *Phys. Chem. Chem. Phys.* **2009**, *11*, 11577.
18. Dragan, E. S.; Bucatariu, F.; Hitruc, G. *Biomacromolecules* **2010**, *11*, 787.
19. Peng, C.; Thio, Y. S.; Gerhardt, R. A.; Ambaye, H.; Lauter, V. *Chem. Mater.* **2011**, *23*, 4548.
20. Gong, X.; Han, L.; Yue, Y.; Gao, J.; Gao, C. *J. Colloid Interface Sci.* **2011**, *355*, 368.
21. Gui, Z.; Qian, J.; Zhao, Q.; Ji, Y.; Liu, Y.; An, Q. *Colloids Surf. A* **2011**, *380*, 270.
22. Dodoo, S.; Balzer, B. N.; Hugel, T.; Laschewsky, A.; Klitzing, R. *Soft Matter* **2013**, *11*, 157.
23. Jian, W.; Xu, S.; Wang, J.; Feng, S. *J. Appl. Polym. Sci.* **2013**, *129*, 2070.
24. Anandhakumar, S.; Gokul, P.; Raichur, A. M. *Mater. Sci. Eng. C* **2016**, *58*, 622.
25. Abdu, S.; Marti-Calatayud, M. C.; Wong, J. E.; Garcia-Gabaldón, Wessling, M. *ACS Appl. Mater. Interfaces* **2014**, *6*, 1843.
26. Deng, H.; Wang, Z.; Zhang, W.; Hu, B.; Zhang, S. *J. Appl. Polym. Sci.* **2015**, *132*, DOI: 10.1002/app.41488.
27. Andreeva, D. V.; Fix, D.; Mohwald, H.; Shchukin, D. G. *J. Mater. Chem.* **2008**, *18*, 1738.
28. Laufer, G.; Kirkland, C.; Morgan, A. B.; Grunlan, J. C. *Biomacromolecules* **2012**, *13*, 2843.
29. Lichter, J. A.; Rubner, M. F. *Langmuir* **2009**, *25*, 7686.
30. Séon, L.; Lavalle, P.; Schaaf, P.; Boulmedais, F. *Langmuir* **2015**, *31*, 12856.
31. Shin, Y.; Cheung, W. H.; Ho, T. T. M.; Bremmell, K. E.; Beattie, D. A. *Phys. Chem. Chem. Phys.* **2014**, *16*, 22409.
32. Karabasz, A.; Bzowska, M.; Lukasiewicz, S.; Bereta, J.; Szczepanowicz, K. *J. Nanopart. Res.* **2014**, *16*, 1.
33. Bucatariu, F.; Ghiorghita, C. A.; Dragan, E. S. *Colloids Surf. B: Biointerfaces* **2015**, *126*, 224.
34. Bucatariu, F.; Ghiorghita, C. A.; Dragan, E. S. *High Perform. Polym.* **2015**, *27*, 563.
35. Xiao, S.; Castro, R.; Marciel, D.; Gonçalves, M.; Shi, X.; Rodrigues, J.; Tomás, H. *Mater. Sci. Eng. C* **2016**, *60*, 348.
36. Zhao, Q.; Qian, J.; An, Q.; Du, B. *J. Mater. Chem.* **2009**, *19*, 8448.
37. Huang, X.; Schubert, A. B.; Chrisman, J. D.; Zacharia, N. S. *Langmuir* **2013**, *29*, 12959.
38. Caridade, S. G.; Monge, C.; Almodóvar, J.; Guillot, R.; Lavaud, J.; Josserand, V.; Coll, J. L.; Mano, J. F.; Picart, C. *Acta Biomater.* **2015**, *15*, 139.
39. Wang, J.; Ren, K.; Chang, H.; Zhang, S.; Jin, L.; Ji, J. *Phys. Chem. Chem. Phys.* **2014**, *16*, 2936.
40. Dubas, S. T.; Farhat, T. R.; Schlenoff, J. B. *J. Am. Chem. Soc.* **2001**, *123*, 5368.
41. Ma, Y.; Sun, J.; Shen, J. *Chem. Mater.* **2007**, *19*, 5058.
42. Ma, Y.; Sun, J. *Chem. Mater.* **2009**, *21*, 898.
43. Chen, D.; Chen, J.; Wu, M.; Tian, H.; Chen, X.; Sun, J. *Langmuir* **2013**, *29*, 8328.
44. Torger, B.; Müller, M. *Spectrochim. Acta A* **2013**, *104*, 546.
45. Giles, C. H.; Smith, D.; Huitson, A. *J. Colloid Interface Sci.* **1974**, *47*, 755.
46. Langmuir, I. *J. Am. Chem. Soc.* **1918**, *40*, 1361.
47. Hall, K.; Eagleton, L. C.; Acrivos, A.; Vermeulen, T. *Indus. Eng. Chem. Fund* **1966**, *5*, 212.
48. Freundlich, H. M. F. *Zeit. Phys. Chem.* **1906**, *57*, 385.
49. Sips, R. *J. Chem. Phys.* **1948**, *16*, 490.
50. Dubinin, M. M. *Chem. Rev.* **1960**, *60*, 235.
51. Tempkin, M. I.; Pyzhev, V. *Acta Phys. Chim. USSR* **1940**, *12*, 327.
52. Dragan, E. S.; Apopei Loghin, D. F.; Cocarta, A. I. *ACS Appl. Mater. Interfaces* **2014**, *6*, 16577.
53. Korsmeyer, R. W.; Lustig, S. R.; Peppas, N. A. *J. Polym. Sci. B: Polym. Phys.* **1986**, *24*, 395.
54. Dragan, E. S.; Bucatariu, F. *Colloids Surf. A* **2016**, *489*, 46.
55. Higuchi, T. *J. Pharm. Sci* **1963**, *52*, 1145.

SGML and CITI Use Only
DO NOT PRINT